

## First Principles Modeling of Tunnel Magnetoresistance of Fe/MgO/Fe Trilayers

Derek Waldron,<sup>1</sup> Vladimir Timoshevskii,<sup>1</sup> Yibin Hu,<sup>2,1</sup> Ke Xia,<sup>2,1</sup> and Hong Guo<sup>1,2</sup>

<sup>1</sup>Centre for the Physics of Materials and Department of Physics, McGill University, Montreal, PQ, H3A 2T8, Canada

<sup>2</sup>International Center for Quantum Structures (ICQS), Institute of Physics, Chinese Academy of Science, Beijing, China

(Received 30 April 2006; published 29 November 2006)

We report *ab initio* calculations of nonequilibrium quantum transport properties of Fe/MgO/Fe trilayer structures. The zero bias tunnel magnetoresistance is found to be several thousand percent, and it is reduced to about 1000% when the Fe/MgO interface is oxidized. The tunnel magnetoresistance for devices without oxidization reduces monotonically to zero with a voltage scale of about 0.5–1 V, consistent with experimental observations. We present an understanding of the nonequilibrium transport by investigating microscopic details of the scattering states and the Bloch bands of the Fe leads.

DOI: 10.1103/PhysRevLett.97.226802

PACS numbers: 85.35.-p, 72.25.-b, 85.65.+h

Since the prediction and elegant physics explanation [1,2] that the magnetic tunnel junction (MTJ) of the Fe/MgO/Fe trilayer structure may have very high tunnel magnetoresistance (TMR), the MgO-based MTJ has progressed at a rapid pace in recent years and produced the highest measured TMR at room temperature: Several groups [3,4] reported a TMR ratio in the range of 180%–250%. The TMR effect presents an excellent opportunity for spintronics; it is the key to magnetoresistive random-access memory [5], programmable logic elements [6], and magnetic sensors.

Atomistic calculations [1,2] have so far played a vital role in elucidating the reason behind the observed large TMR in Fe/MgO/Fe MTJs [1–4]. There are, however, a number of important issues remaining to be understood from atomic first principles. Most existing work predicted [1,2] TMR to be greater than 1000%; experimental data are still lower. More serious is that experimental data on MgO-based MTJs show a monotonically *decreasing* TMR as a function of applied bias voltage [3,4], and it reduces to zero when the bias is about 1 V. To the best of our knowledge, there have been two atomistic calculations of bias dependence of TMR for MgO barriers [7,8]; both used the Korringa-Kohn-Rostoker numerical technique. Reference [7] predicted a substantial *increase* of TMR versus bias for the asymmetric system analyzed there, while Ref. [8] found a roughly constant TMR, a decaying TMR, or an entirely negative TMR versus bias depending on atomic structures of the interface. Earlier theory [9] on Al<sub>2</sub>O<sub>3</sub>-based MTJs has attributed the small bias dependence of magnetoresistance to magnon scattering. Given the importance of MgO-based MTJs, further *quantitative* understanding on quantum transport in Fe/MgO/Fe at a finite bias is necessary.

Here we present a first principles atomistic analysis of nonequilibrium quantum transport in the Fe/MgO/Fe MTJ. We use a state-of-the-art quantum transport technique [10,11] which is based on real-space, Keldysh nonequilibrium Green's function (NEGF) formalism combined with density functional theory (DFT). The basic idea of the NEGF-DFT formalism [10] is to calculate the

device Hamiltonian and electronic structure by DFT, populate this electronic structure using NEGF, which properly takes into account nonequilibrium quantum statistics, and deal with open device boundaries directly using real-space numerical techniques. Our results show that, for the fully relaxed atomic structure of the Fe/MgO/Fe device, the zero bias equilibrium TMR ratio reaches several thousand percent—consistent with previous theoretical results [1,12]. This value is drastically reduced to about 1000% if the Fe/MgO interfaces are oxidized by 50% oxygen. We found that the TMR ratio is quenched by bias voltage  $V_b$  with a scale of about 1 V.

The MTJ is schematically shown in Fig. 1(a), where a number of MgO(100) layers are sandwiched by two Fe(100) leads. The MTJ is periodic in the  $x$ - $y$  direction, while the leads also extend to  $z = \pm\infty$  (transport direction). For DFT, we use standard norm-conserving pseudopotentials [13] and an  $s$ ,  $p$ ,  $d$  double-zeta LCAO basis set

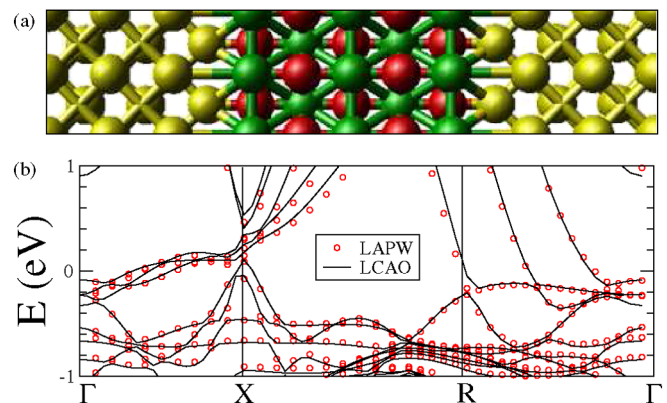


FIG. 1 (color online). (a) Schematic plot of a two-probe Fe(100)/MgO(100)/Fe(100) device. The system has infinite extent in the  $(x, y)$  direction with a lattice constant of 2.82 Å and extends to  $\pm\infty$  in the  $z$  direction. (b) Band structure of a periodic  $\cdots$ Fe/MgO/Fe/MgO $\cdots$  lattice obtained using optimized LCAO pseudopotentials and basis sets compared to that from the full potential LAPW method. A good agreement is found to be necessary in order to carry out the NEGF-DFT analysis for the two-probe Fe/MgO/Fe devices.

[14]. The exchange-correlation potential is treated at the local spin density approximation level. In order to accurately determine transport properties of the MTJs, we found that special care must be given to the pseudopotentials and basis sets. In our work, these inputs were carefully constructed to accurately reproduce the electronic structures of Fe, MgO, and the periodic lattice of the Fe/MgO interface obtained by the full potential linear augmented-plane-wave (LAPW) method [15]. The latter comparison is shown in Fig. 1(b).

For the two probe MTJ simulation, we found that  $20 \times 20$  ( $k_x, k_y$ ) points suffice to sample the 2D transverse Brillouin zone (BZ) for converging the density matrix on the *complex contour* energy integration in the NEGF-DFT self-consistent analysis [10]. Much denser  $k$  sampling, up to  $10^6$  ( $k_x, k_y$ ) points, was required to converge the density matrix for the real energy integration of NEGF [10,11] and for computing the transmission coefficient by summing over the BZ:  $T_\sigma(E, V_b) = \sum_{k_x, k_y} T_\sigma^{k_x, k_y}(E, V_b)$ . Here  $E$  is the electron energy, and  $V_b$  is the external bias. The BZ resolved transmission  $T_\sigma^{k_x, k_y}$  is obtained by the standard Green's functions technique:  $T_\sigma^{k_x, k_y} \equiv \text{Tr}[\text{Im}(\Sigma_L^r) \times \mathbf{G}^r \text{Im}(\Sigma_R^r) \mathbf{G}^a]$ , where all quantities in the trace are functions of transverse momentum. Here  $\sigma \equiv \uparrow, \downarrow$  is the spin index,  $\mathbf{G}^{r,a}$  are the retarded or advanced Green's function matrices in spin and orbital space, and  $\Sigma_{L,R}^r$  are the retarded self-energies due to the existence of the bulk-3D left or right Fe leads. Finally, the spin current (spin polarized charge current) is obtained by  $I_\sigma(V_b) = \frac{e}{h} \times \int_{\mu_L}^{\mu_R} dE T_\sigma(E, V_b) [f_L(E - \mu_L) - f_R(E - \mu_R)]$ , where  $\mu_{L,R}$  is the electrochemical potential of the left or right leads. The total charge current is given by  $I \equiv I_\uparrow + I_\downarrow$ . In all our calculations, the atomic structure was fully relaxed by the LAPW [15] method between three Fe layers on each side of the MgO, with the most remote layer of Fe atoms fixed at crystalline positions during relaxation. The  $x$ - $y$  lattice constant  $a$  of the interface was fixed to our *calculated* one for bcc Fe,  $a = 2.82 \text{ \AA}$ . The Fe-O distance was found to be  $2.236 \text{ \AA}$  for a completely relaxed structure in agreement with previous studies [1].

Figures 2(a) and 2(b) plot the current-voltage ( $I$ - $V$ ) characteristics (solid line) for a 5-layer MgO device in the parallel magnetization configuration (PC) and the anti-parallel configuration (APC) of the two Fe leads, respectively. The lower insets plot the majority spin current at a small bias range. For a bias less than 0.8 V, the total current remains extremely small. At about 1.5 V, the device ‘‘turns on,’’ and current increases rapidly afterward. Such a turn-on voltage is consistent with experimental data [4,16]. The spin currents are shown as the dashed and dotted lines for the up and down channels (majority and minority channels), respectively. We found that the initial rise of the current at  $\sim 0.8 \text{ V}$  in the PC is dominated by the down channel where  $I_\downarrow$  exceeds  $I_\uparrow$  by over a factor of 8. This can be explained by investigating the transmission coefficients

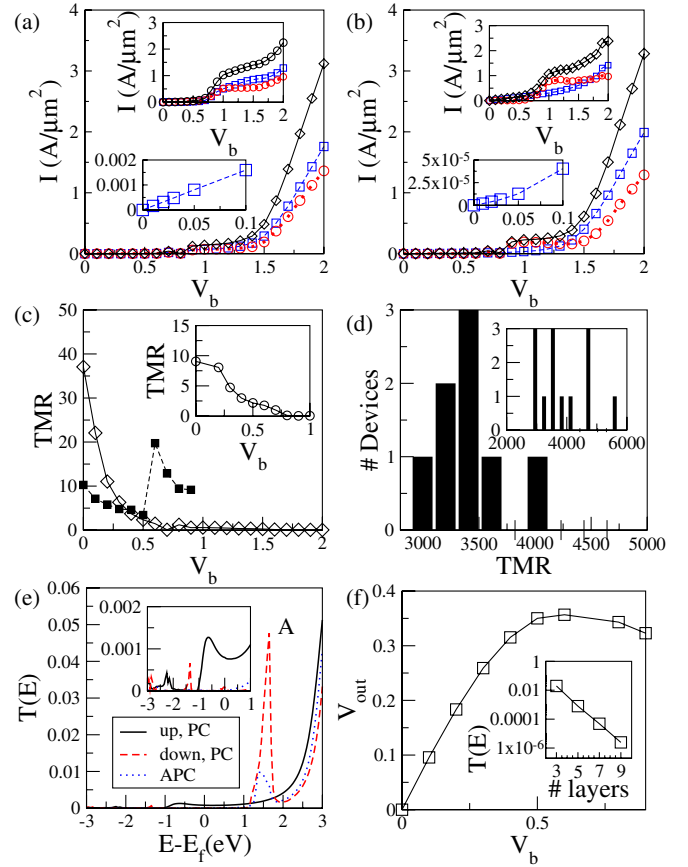


FIG. 2 (color online). (a),(b)  $I$ - $V$  curves for the 5-layer PC and APC, respectively. Solid line (diamonds): total current; dashed line (squares):  $I_\uparrow$ ; dotted line (circles):  $I_\downarrow$ . Upper inset:  $I$ - $V$  curves for a 3-layer device. Lower inset: majority current  $I_\uparrow$  vs  $V_b$  for small ranges of  $V_b$ . (c) TMR vs bias  $V_b$  for a 5-layer device (diamonds). The solid squares are data for 50% oxidation of the two Fe/MgO interfaces. Inset: TMR for a 3-layer device. (d) Histogram of TMR for several 5-layer devices with a variation in the position of the surface atoms. Inset: Histogram for varying all of the Mg and O atoms in the device. (e) Transmission coefficient  $T_\sigma$  versus energy  $E$  for  $V_b = 0$ .  $E = 0$  is the Fermi energy of leads. Solid line:  $T_\uparrow$  for PC setup; dashed line:  $T_\downarrow$  for the PC; dotted line:  $T_\uparrow = T_\downarrow$  for the APC. Inset: The same transmission coefficients at energies between  $-3$  and  $1 \text{ eV}$ . (f) The magnitude of the output signal modulation  $V_{\text{out}}$  as a function of bias. Inset: Semilog plot of zero bias total transmission coefficients  $T$  versus the number of MgO layers for PC setup, indicating an exponential decrease of  $T$ .

(see below). Above  $\sim 1.5 \text{ V}$ , the spin currents roughly contribute equally to the total current. The  $I$ - $V$  curves for a 3-layer MgO device are plotted in the inset in Figs. 2(a) and 2(b) and show similar features.

From the  $I$ - $V$  curves, we infer a TMR ratio using the common definition:  $R_{\text{TMR}} \equiv (I_{\text{APC}} - I_{\text{PC}})/I_{\text{APC}}$ , where  $I_{\text{APC,PC}}$  are the total currents in APC and PC, respectively. At  $V_b = 0$  when all currents vanish, we compute  $R_{\text{TMR}}$  use transmission coefficients [17]. From Fig. 2(c), for a 5-layer MgO device,  $R_{\text{TMR}} \sim 3700\%$  at zero bias and declines with  $V_b$  essentially vanishes on a scale of about 1 V. For the 3-

layer MgO, we found  $R_{\text{TMR}} \sim 850\%$  at zero bias and declines to zero with  $V_b$  on a similar bias scale. The present experimental TMR values are significantly lower than these and other [1,2] theoretical predictions. It is anticipated that surface roughness may play a role [18]. To investigate this effect, we generated eight atomic structures of 5-layer MgO: For each device, we varied the  $z$  coordinates of the surface Mg and O atoms from their relaxed positions, by a random displacement corresponding to about 1% of the bond length. NEGF-DFT analysis is carried out for them and results are shown in Fig. 2(d): The minimum TMR is about 3000% while the maximum is  $\sim 4000\%$ , with an average of 3580%. Although the sample size is small and a random change of bond length may not reflect experimental reality, the TMR ratio does change due to small interface atom displacements. A similar analysis is carried out for 13 5-layer MgO devices where all the Mg and O atoms were displaced randomly by roughly 1% of the bond length; the result is in the inset in Fig. 2(d). We found that more drastic changes of zero bias TMR are obtained when the two Fe/MgO interfaces are oxidized [19]. For two 5-layer MgO atomic structures with 100% and 50% oxygen at the interfaces [20], the zero bias TMR is dropped to  $\sim 169\%$  and  $\sim 1000\%$ , respectively. The reason for this drop is found to be due to a decrease of PC current while the APC current remains at a similar value to that of unoxidized interfaces, consistent with the conclusion of Ref. [21].

Figure 2(c) shows a dramatic quench of TMR by the external bias voltage with a scale of about 1 V, in agreement with the experimental data [4,22]. The origin of the TMR quenching is due to a very fast rise in the APC current relative to the PC current as a function of bias. We now analyze these features. First, the voltage dependence of the total current and spin current [Figs. 2(a) and 2(b)] can be understood from the behavior of the transmission coefficient  $T_\sigma$ . Figure 2(e) plots  $T_\sigma = T_\sigma(E)$  versus electron energy  $E$  at zero bias for the PC and APC of the 5-layer MgO device. In the PC, the majority carrier transmission  $T_\uparrow$  (solid line) is smooth and several orders of

magnitude larger than  $T_\downarrow$  (dashed line) when  $E$  is near the Fermi energy of the leads ( $E_f = 0$ ). By analyzing the spin-dependent scattering states [10] of the MTJ, we were able to determine which bands of the Fe leads contribute to the transmission. We found that  $T_\uparrow$  is dominated by the  $\Delta_1$  band of the Fe leads, in agreement with Ref. [1]. Below  $-1$  eV,  $T_\uparrow$  becomes extremely small due to the disappearance of the  $\Delta_1$  band.  $T_\downarrow$ , on the other hand, is considerably less smooth because the transmission near the Fermi level is mostly dominated by interface resonance states [23]. In particular, a large peak in  $T_\downarrow$  appears above  $E = 1$  eV: As  $E$  is increased, different Fe bands may participate in transport, and this peak is due to such a contribution. This  $T_\downarrow$  peak explains the much larger minority-channel current than the majority-channel current in PC at  $V_b = 0.8$  V [Fig. 2(a)], as already noted above.

Second, for APC, we obtain  $T_\uparrow = T_\downarrow$  for all  $E$  at zero bias due to the geometrical symmetry of the device [dotted line in Fig. 2(e)]. We found that the BZ resolved total transmission  $T^{k_x, k_y}(E, V_b) = T_\uparrow^{k_x, k_y} + T_\downarrow^{k_x, k_y}$ , shown in Fig. 3(c) for  $V_b = 0$  and Fig. 3(d) for  $V_b = 0.05$  V, is dominated by broad and smooth peaks at around  $|k_x| = |k_y| = 0.12$  (in units of  $\pi/a$  throughout the Letter, where  $a$  is the Fe lattice constant mentioned above), and there is almost no transmission at  $k_x = k_y = 0$ . For  $V_b = 0$ , Fig. 3(c) also shows that the dominating peaks are surrounded by other much sharper peaks. For the APC, it is the majority channel from one Fe layer traversing the MgO barrier and going to the minority channel in the other Fe layer. Figures 3(a) and 3(b) plot the majority and minority electronic band structures of Fe near  $E_f$  for  $|k_x| = |k_y| = 0.12$ , respectively. By projecting scattering states with  $|k_x| = |k_y| = 0.12$  onto the Fe bands in Figs. 3(a) and 3(b), the dominating peaks are found to be largely due to channel transmission: They are due to the band labeled “1” in Fig. 3(a) at one Fe contact transmitting to the band labeled “2” on the other Fe contact. Our calculations show that this band-to-band transmission contributes  $2.37 \times 10^{-4}$  to majority channel  $T_\uparrow^{k_x, k_y}$ . Other band-to-band transmissions are considerably

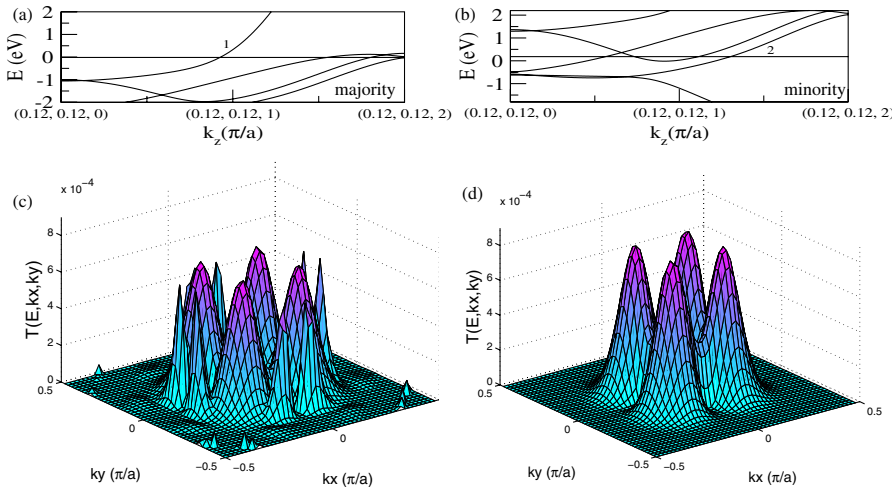


FIG. 3 (color online). (a),(b) Fe bands at  $|k_x| = |k_y| = 0.12\pi$  versus  $k_z$  for majority and minority electrons, respectively. (c),(d) Total BZ resolved transmission coefficient at  $E_f$  versus  $k_x, k_y$ , for 5-layer MgO (c) for  $V_b = 0$  and (d) for  $V_b = 0.05$  V. The dominant peaks are near  $|k_x| = |k_y| = 0.12$ .

smaller. Similarly,  $T_{\uparrow}^{k_x, k_y}$  is mainly contributed from band 2 to band 1. Therefore, it is the band-to-band transmissions which give almost the entire height of the dominating peaks in Fig. 3(c) [note Figs. 3(c) and 3(d) plot the total BZ resolved transmission] [24].

Third, we found that bias voltage has dramatic effects for the APC. The very sharp peaks in Fig. 3(c), which are due to interface resonances occurring at zero bias, are completely removed by a finite bias of 0.05 V, as shown in Fig. 3(d). Moreover, the dominating peaks become considerably higher than those in Fig. 3(c). We checked that even 0.01 V bias can remove these sharp resonances. This is likely due to the very small widths of interface resonances, as predicted by Ref. [23]. Again, we found that transmission from band 1 of the left Fe lead to band 2 of the right lead dominates  $T_{\uparrow}^{k_x, k_y}$ , contributing  $3.2 \times 10^{-4}$  to the peaks. This value is considerably larger than the value at zero bias, indicating that the bias enhances the coupling of Fe bands across the MgO barrier for the APC, causing a fast relative increase in the APC current as a function of bias voltage, and is responsible for quenching the TMR observed in Fig. 2(c). Finally, the solid squares in Fig. 2(c) show the TMR vs bias for the 50% oxidized Fe/MgO interfaces: It also decreases with bias until  $V_b \sim 0.5$  V. After this bias, we observe an increase of TMR for the oxidized interface: Additional calculations showed that this increase is due to the presence of a new resonance formed just above the Fermi level for the spin up channel caused by the Fe-O interaction in the oxidization plane.

An important parameter is the magnitude of the output signal modulation, namely,  $V_{\text{out}} \equiv V_b(R_{\text{APC}} - R_{\text{PC}})/R_{\text{APC}}$ , with  $V_b$  the applied bias and  $R_{\text{APC}}$  and  $R_{\text{PC}}$  the junction resistances for the APC and the PC, respectively.  $V_{\text{out}}$  is plotted as a function of bias in Fig. 2(f): It increases in a roughly linear manner and then bends over at around  $V_b \sim 0.5$ – $0.7$  V, where  $V_{\text{out}}$  is about 350 mV. These voltage scales are rather similar to the experimental data [4,22]. Finally, the inset in Fig. 2(f) shows a semilog plot of the zero bias total transmission at Fermi energy versus four thicknesses of the MgO barrier for the PC, and the data are in perfect consistency with the physics of tunneling.

In summary, we have analyzed nonequilibrium quantum transport properties of Fe/MgO/Fe MTJs from atomic first principles without any phenomenological parameter. The obtained voltage scales for transport features are consistent with experimental data; these include the turning on voltage for currents, the voltage scale for TMR quenching, the maximum value of  $V_{\text{out}}$ , as well as the turning over voltage of  $V_{\text{out}}$ . The quench of TMR by bias is found to be due to a relatively fast increase of channel currents in the APC. Very large TMR at zero bias is obtained which is substantially reduced by oxidization of the Fe/MgO interfaces.

We gratefully acknowledge financial support from NSERC of Canada, FRQNT of Quebec, CIAR, a Killam Research grant (H. G.), and NSF-China (K. X.). We thank Dr. Lei Liu for assistance in several useful analysis soft-

ware tools, Dr. Eric Zhu for his participation at early stages of this work, and Dr. Xiaoguang Zhang for illuminating communications on TMR physics.

- 
- [1] W.H. Butler, X.-G. Zhang, T.C. Schulthess, and J.M. MacLaren, Phys. Rev. B **63**, 054416 (2001).
  - [2] J. Mathon and A. Umerski, Phys. Rev. B **63**, 220403(R) (2001).
  - [3] S. S. P. Parkin *et al.*, Nat. Mater. **3**, 862 (2004).
  - [4] S. Yuasa *et al.*, Nat. Mater. **3**, 868 (2004).
  - [5] J. S. Moodera, L. R. Kinder, T. M. Wong, and R. Meservey, Phys. Rev. Lett. **74**, 3273 (1995); T. Miyazaki and N. Tezuka, J. Magn. Magn. Mater. **139**, L231 (1995).
  - [6] A. Ney, C. Pampuch, R. Koch, and K.H. Ploog, Nature (London) **425**, 485 (2003).
  - [7] C. Zhang *et al.*, Phys. Rev. B **69**, 134406 (2004).
  - [8] C. Heiliger, P. Zahn, B. Yu Yavorsky, and I. Mertig, Phys. Rev. B **72**, 180406(R) (2005).
  - [9] S. Zhang, P.M. Levy, A.C. Marley, and S.S.P. Parkin, Phys. Rev. Lett. **79**, 3744 (1997).
  - [10] J. Taylor, H. Guo, and J. Wang, Phys. Rev. B **63**, 245407 (2001); **63**, 121104 (2001).
  - [11] D. Waldron, P. Haney, B. Larade, A. MacDonald, and H. Guo, Phys. Rev. Lett. **96**, 166804 (2006).
  - [12] C. Tusche *et al.*, Phys. Rev. Lett. **95**, 176101 (2005); J.P. Velev, K.D. Belashchenko, and E.Y. Tsympal, Phys. Rev. Lett. **96**, 119601 (2006).
  - [13] N. Troullier and J.L. Martins, Phys. Rev. B **43**, 1993 (1991).
  - [14] J.M. Soler *et al.*, J. Phys. Condens. Matter **14**, 2745 (2002).
  - [15] P. Blaha, *et al.*, WIEN2K, An Augmented Plane Wave + Local Orbitals Program for Calculating Crystal Properties (TU Wien, Austria, 2001), ISBN 3-9501031-1-2.
  - [16] W. Wulfhekel *et al.*, Appl. Phys. Lett. **78**, 509 (2001).
  - [17] For a 3-layer MgO at zero bias, the majority transmission coefficient at  $k_x = k_y = 0$  is found to be 0.44. This value can be compared with that obtained using the full-potential linear augmented-plane-wave method (FLAPW) and embedding Green's function method which gave  $\sim 0.4$ . E. Wortmann, G. Bihlmayer, and S. Blügel, J. Phys. Condens. Matter **16**, S5819 (2004).
  - [18] P.X. Xu *et al.*, Phys. Rev. B **73**, 180402(R) (2006).
  - [19] H.L. Meyerheim *et al.*, Phys. Rev. Lett. **87**, 076102 (2001).
  - [20] The atomic structure with oxidization is also relaxed using FLAPW.
  - [21] X.-G. Zhang, W.H. Butler, and A. Bandyopadhyay, Phys. Rev. B **68**, 092402 (2003).
  - [22] C. Tiusan *et al.*, Appl. Phys. Lett. **88**, 062512 (2006).
  - [23] O. Wunnicke *et al.*, Phys. Rev. B **65**, 064425 (2002).
  - [24] The bands in Figs. 3(a) and 3(b) are at  $|k_x| = |k_y| = 0.12$  where the APC transmission has the broad peaks [Figs. 3(c) and 3(d)]. On the other hand, we refer to bands at  $k_x = k_y = 0$  as  $\Delta_1$  bands, etc. In this sense, band 1 in Fig. 3(a) is rather like the  $\Delta_1$  band, while band 2 in Fig. 3(b) is like the  $\Delta_5$  band. Coupling between these bands in APC is possible due to  $|k_x| = |k_y| \neq 0$  and due to scattering at the interfaces.